The Dark Energy Survey and Operations: Year 1

H. T. Diehl[1a], T. M. C. Abbott[b], J. Annis[a], R. Armstrong[c], L. Baruah[d], A. Bermeo[d], G. Bernstein[c], E. Beynon[e], C. Bruderer[f], E. J. Buckley-Geer[a], H. Campbell[e], D. Capozzi[e], M. Carter[d], R. Casas[g], L. Clerkin[h], R. Covarrubias[i], C. Cuhna[j], C. D'Andrea[e], L. da Costa[k], R. Das[l], D. L. DePoy[m], J. Dietrich[n,o], A. Drlica-Wagner[a], A. Elliott[p], T. Eifler[c], J. Estrada[a], J. Etherington[e], B. L. Flaugher[a], J. Frieman[a], A. Fausti Neto[k], M. Gelman[i], D. Gerdes[l], D. Gruen[n,q], R. Gruendl[i,r], J. Hao[a], H. Head[s], J. Helsby[t], K. Hoffman[g], K. Honscheid[p], D. James[b], M. Johnson[i], T. Kacprzac[h], J. Katsaros[d], R. Kennedy[d], S. Kent[a], R. Kessler[t], A. Kim[u], E. Krause[c], R. Kron[a], S. Kuhlmann[v], A. Kunder[b], T. Li[m], H. Lin[a], N. Maccrann[w], M. March[c], J. Marshall[m], E. Neilsen[a], P. Nugent[u], P. Martini[x], P. Melchior[o,x], F. Menanteau[i,r], R. C. Nichol[e], B. Nord[a], R. Ogando[k,y], L. Old[z], A. Papadopoulos[e], K. Patton[x], D. Petravick[i], A. A. Plazas[aa], R. Poulton[d], A. Pujol[g], K. Reil[j], T. Rigby[d], K. Romer[d], A. Roodman[j], P. Rooney[d], E. Sanchez Alvaro[ab], S. Serrano[g], E. Sheldon[aa], A. Smith[s], R. C. Smith[b], M. Soares-Santos[a], M. Soumagnac[h], H. Spinka[v], E. Suchyta[p], D. Tucker[a], A. R. Walker[b], W. Wester[a], M. Wiesner[a], H. Wilcox[e], R. Williams[d], B. Yanny[a], Y.-Y. Zhang[l]

[a]Fermi National Accelerator Laboratory, P.O. Box 500, Batavia, IL,60510 USA; [b]National Optical Astronomy Observatory, Cerro Tololo Inter-American Observatory, Casilla 603, La Serena, Chile; [c]Dept. of Physics and Astronomy, University of Pennsylvania, Philadelphia, PA, 19104 USA; [d]Dept. of Physics and Astronomy, Sussex, UK; [e]Institute of Cosmology and Gravitation, University of Portsmouth, Portsmouth, PO1 3FX, UK; [f]Institute for Astronomy, Department of Physics, ETH Zurich, Wolfgang-Pauli-Srasse 27, CH-8093 Zurich, Switzerland; [g]Institut de Ciéncies de l'Espai (ICE, IEEC/CSIC), E-08193 Bellaterra (Barcelona), Spain; [h]Dept. of Physics and Astronomy, University College London, Gower St., London, WC1E 6BT, UK; [i]National Center for Supercomputing Applications, 1205 West Clark St., Urbana, IL 61801, USA; [j]Kavli Institute for Particle Astrophysics and Cosmology, 452 Lomita Mall, Stanford University, Stanford, CA, 94305 USA; [k]Laboratório Interinstitucional de e-Astronomia - LIneA, Rua Gal. José Cristino 77, Rio de Janeiro, RJ - 20921-400, Brazil; [l]Department of Physics, University of Michigan, Ann Arbor, MI, 48109 USA; [m]George P. and Cynthia Woods Mitchell Institute for Fundamental Physics and Astronomy, and Department of Physics and Astronomy, Texas A&M University, College Station, TX 77843, USA; [n]University Observatory Munich, Scheinerstrasse 1, 81679 Munich, Germany; [o]Excellence Cluster Universe, 85748 Garching b. Munich, Germany; [p]Dept. of Physics, The Ohio State University, Columbus, OH, 43210 USA; [q]Max Planck Institute for Extraterrestrial Physics, Giessenbachstrasse, 85748 Garching, Germany; [r]Department of Astronomy, University of Illinois at Urbana-Champaign, W. Green Street, Urbana, IL 61801, USA; [s]Dept. of Physics and Astronomy, Austin Peay State University, Clarksville, TN, 37044 USA; [t]Kavli Institute for Cosmological Physics, University of Chicago, Chicago, IL 60637 USA; [u]Lawrence Berkeley National Laboratory, 1 Cyclotron Road, Berkeley, CA 94720, USA; [v]Argonne National Laboratory, 9700 South Cass Ave., Lemont, IL, 60439 USA; [w]Jodrell Bank Center for Astrophysics, School of Physics and Astronomy, University of Manchester, Oxford Road, Manchester, M13 9Pl, UK; [x]Center for Cosmology and Astro-Particle Physics, The Ohio State University, Columbus, OH, 43210 USA; [y]Observatório Nacional, R. Gal. José Cristino 77, BR Rio de Janeiro, RJ 20921-400, Brazil; [z]Cripps Centre for Astronomy and Particle Theory, University Park, Nottingham, NG7 2RD, UK;

[1] Diehl@FNAL.GOV; phone 1-630-840-8307.

[aa]Brookhaven National Laboratory, Building 510, Upton, NY, 11973 USA; [ab]Centro de Investigaciones Energéticas, Medioambientales y Tecnológicas (CIEMAT), Madrid, Spain

ABSTRACT

The Dark Energy Survey (DES) is a next generation optical survey aimed at understanding the accelerating expansion of the universe using four complementary methods: weak gravitational lensing, galaxy cluster counts, baryon acoustic oscillations, and Type Ia supernovae. To perform the 5000 sq-degree wide field and 30 sq-degree supernova surveys, the DES Collaboration built the Dark Energy Camera (DECam), a 3 square-degree, 570-Megapixel CCD camera that was installed at the prime focus of the Blanco 4-meter telescope at the Cerro Tololo Inter-American Observatory (CTIO). DES started its first observing season on August 31, 2013 and observed for 105 nights through mid-February 2014. This paper describes DES "Year 1" (Y1), the strategy and goals for the first year's data, provides an outline of the operations procedures, lists the efficiency of survey operations and the causes of lost observing time, provides details about the quality of the first year's data, and hints at the "Year 2" plan and outlook.

Keywords: Cosmology, Dark Energy Survey, Dark Energy Camera, Operations, CTIO

1. INTRODUCTION

The Dark Energy Survey (DES) is an international collaboration, with over 200 scientists from over 20 institutions in the US, the UK, Spain, Brazil, Switzerland, and Germany. The DES [1-2] will measure dark energy parameters using four complementary techniques: galaxy cluster counting, baryon acoustic oscillations, weak gravitational lensing, and Type Ia supernovae. The wide-field (WF) survey will produce images of 5000 square degrees of the southern galactic cap collected during 525 nights of observing from 2013 to 2018. The WF survey will be accomplished in 10 dither patterns (tilings). Ten 3-square-degree fields will be imaged repeatedly to produce a supernovae survey. In order to carry out these surveys, the DES Collaboration constructed a new instrument, the Dark Energy Camera.

The Dark Energy Camera (DECam) [3-7] was designed and built from 2004 to 2010. The camera uses 5 fused-silica optical elements to attain an f/2.7, 2-degree-wide image on the focal plane. The focal plane itself has 42 cm radius and is populated with 62 2048x4096 pixel 250 μm thick, fully-depleted, red-sensitive CCDs [8], for imaging. It was first assembled and tested at Fermilab on a full-scale reproduction of the telescope top-rings that we called the "Telescope Simulator" [9-10]. It was delivered to CTIO in a series of shipments starting in early 2010. The imager was the last major component to be shipped [11], arriving in December 2011.

CTIO led [12-13] the camera installation with intense and active participation by the DECam design and construction team. Installation started in January 2011 with the setup of the new f/8 handling system, necessary because the inner top-end ring would no longer be able to pivot 180 degrees on its axle (thus facing the f/8 mirror towards the primary mirror) after DECam was installed. From June to August 2011 the camera infrastructure was installed into the Blanco Dome, including the LN2 system that cools the CCDs to operating temperature [14], and the chillers for the readout electronics. Starting in February 2012 the old Prime Focus cage was removed and the new DECam cage and optical corrector, "the barrel", were installed. Over the next months the support services for the camera were installed onto the telescope and the mountain top computer system was installed and tested. The imager was attached to the barrel on August 30th. The filter-changer and shutter were installed on September 6th. "Official First Light" was achieved on September 12, 2012 [15]. DECam achieved 0.8" seeing across the focal plane within 45 minutes of its first exposure. Fig. 1 shows a photo of the Dark Energy Camera mounted at the Prime Focus of the Blanco telescope.

DECam was commissioned during September and October 2012. During that period the active-optics "focus" system [16-17] and the guide-star system [6] were enabled and debugged. A survey and instrument testing period called "Science Verification" was carried out by the DES Collaboration and "Community Astronomers" during November. Regular "Community Observing" began on December 1, 2012. Primarily because of concerns over elongation of the images due to telescope tracking oscillations, principally in RA [18], Science Verification was extended into 2013 and the first observing season for DES was postponed. The image quality problems were finally resolved in late January when the RA bearing oil-scraper was set to the proper clearance and the Primary Mirror cooling system was enabled. Science Verification ended after the night of February 22, 2013. For the period December 1, 2012 to February 28, 2013,

the Community Observers and DES equally divided the 80 nights of telescope time. After that, the camera was used by the astronomical community. May and July 2013 brought "hardening" of camera infrastructure systems including the liquid-nitrogen (LN2) pump and the front-end electronics cooling, which had unexpected failures. This work was carried-out by technical staff from Fermilab and CTIO and is part of the training of the CTIO staff in some unfamiliar technologies. DES scientists participated in the planning and analysis of camera and telescope engineering observations throughout this period. DES continues to investigate improvements to the LN2 pump operation so that those will not need to be replaced at the cost of at least 2-3 nights of operations every 7 months. The first observing season of the Dark Energy Survey started on August 31, 2013.

This paper describes DES "Year 1" (Y1), the strategy and goals for the first year's data, provides an outline of the operations procedures, lists the efficiency of survey operations and the causes of lost observing time, provides details about the quality of the first year's data, and hints at the "Year 2" plan and outlook.

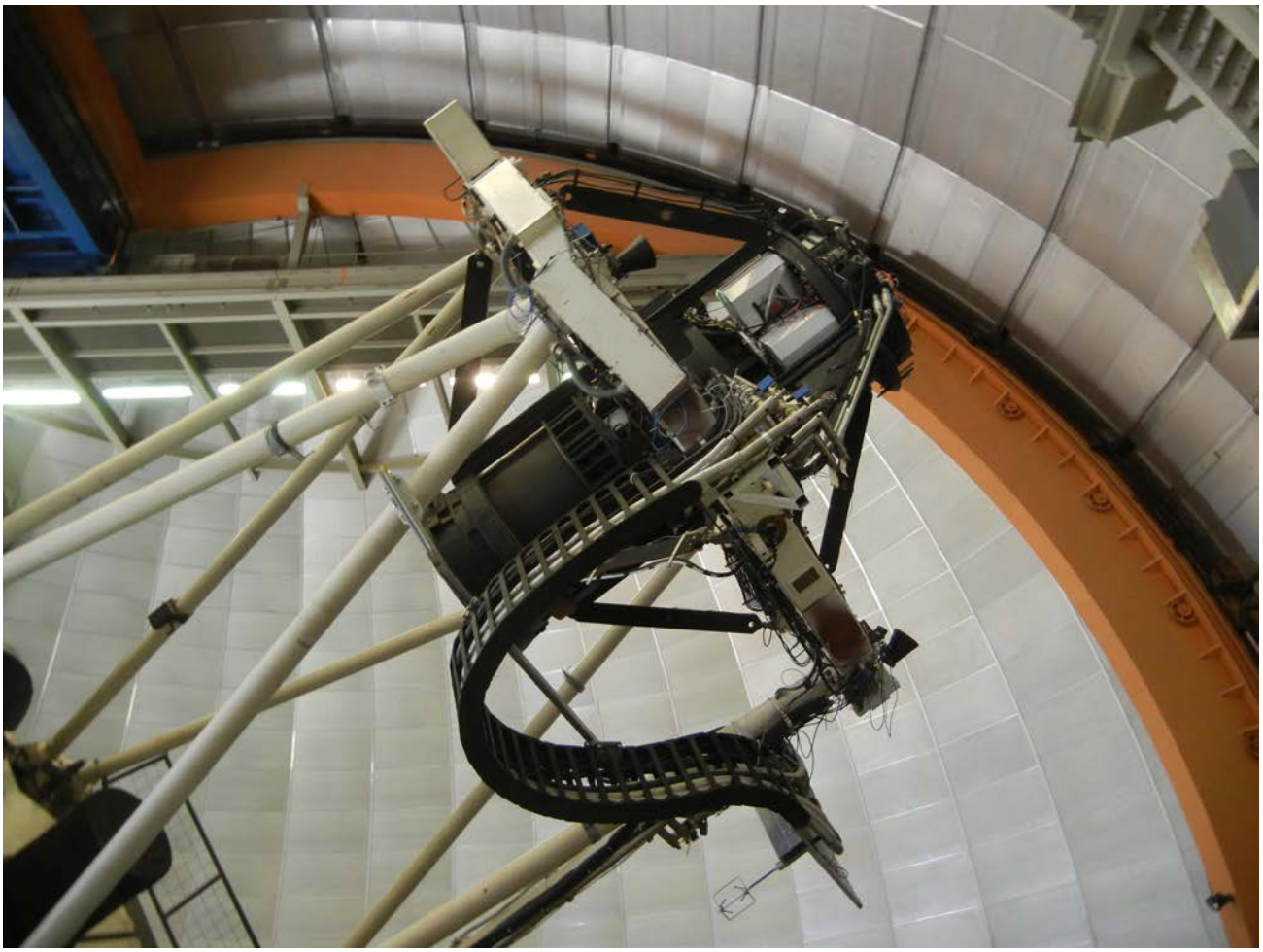

Figure 1. The Dark Energy Camera is mounted at the Prime Focus of the Blanco 4m telescope at CTIO. The Primary Mirror is just out of the photo, low and to the left. The camera assembly is approximately 14 feet long and is secured to the inner telescope ring. The aluminum covers of three of the four readout electronics crates are visible on the upper right, as is the stiff cable tray dangling from the inner ring and supported by the telescope truss assembly.

2. YEAR 1 PLAN & OPERATIONS PROCEDURE

2.1 The Dark Energy Survey "Year 1" Schedule and Survey Fields

The first Y1 night of DES observing started on the night of August 31, 2013. Y1 concluded during the night that started on February 9, 2014. There were 91 full nights through January 4, 2014 and 28 first-half nights after that, for a total of 105 nights. The western part of the part of the survey field was no longer observable by the end of the run and the eastern part of the survey field was setting in the first half of the night by the end of January. During Y1 there were 17 nights assigned to "Engineering" and these also tended to be during periods of Full Moon. "Community Users" were assigned the remaining 24 full nights and 28 second-half nights during the period Aug. 31st to Feb. 9th.
The 5000 square-degree DES observing "wide-field" (WF) has three main regions. See Fig. 2. There is a broad roughly circular region from RA of roughly 0 to 120 degrees and DEC -70 to -10 degrees that provides a large contiguous area for the large-scale structure measurements. There is a wide roughly box-shaped region around the South Pole Telescope (SPT) observing area [19]. Finally, the survey encompasses a part of SDSS Stripe 82 [20], primarily for calibration purposes.

For Y1 we chose to observe a 2000 square-degree subset of the entire DES footprint. We planned to observe that 2000 square-degrees four times each in each of the five filters, g, r, i, z, and Y-bands. Due to curvature of the sky, gaps between the CCDs, non-functioning CCDs, and edge effects, a single, complete tiling covers approximately 84% of the survey footprint area. The g, r, i, and z-band exposures are 90 seconds duration. The Y-band exposures are 45 seconds duration.

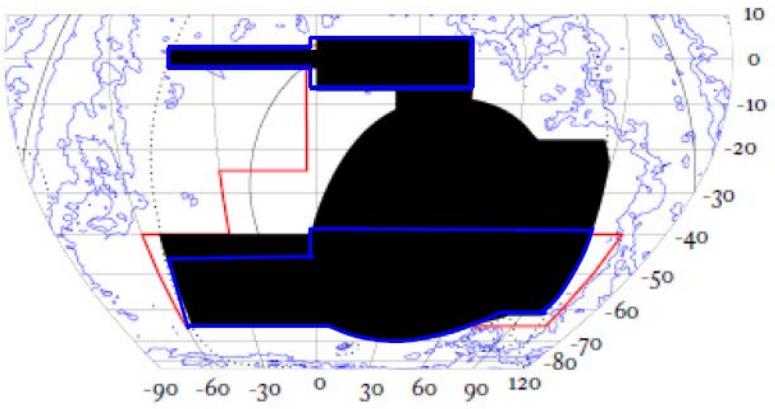

Figure 2. The Dark Energy Survey observing "wide fields" are shown in black on this plot of RA and DEC. During Y1 DES planned to observe the areas outlined in blue, which encompass SDSS Stripe 82 (upper) and the SPT area (lower). The red line is an artifact, showing a previous version of the survey field.

The 10 supernova fields are shown in Table 1. The 8 "shallow fields" are observed for single exposures in g-band (175s), r-band (150s), and i-band (200s) and for two images in z-band (200s each). The limiting magnitudes are 24.9, 24.3, 23.9, and 23.8 for g-, r-, i-, and z-bands, respectively. The 5 exposures of a shallow field are considered a "sequence" and the sequence is observed consecutively. The two "deep fields" are observed for 3 exposures of 200s each in g-band, for 400s each in r-band, for 5 exposures of 360s each in i-band, and for 11 exposures of 330s each in z-band. The exposures in each given filter for the deep fields are considered a sequence. The exposures for each filter are sequential but the different filters might be observed at different times during a single night or on different nights. The limiting magnitudes for the deep field sequences are 25.6, 25.4, 25.1, and 24.8 for g-, r-, i-, and z-bands, respectively. Because the telescope pointing is accurate to 5" to 7" in both RA and DEC, each SN sequence is preceded by a 10s exposure that is processed to find the pointing offset correction applied before the first exposure in the sequence starts.

Table 1. RA and DEC (J2000) of the 10 DES supernova fields. Fields C3 and X3 are “deep fields”. The other 8 fields are “shallow fields”.

Field Name	RA	DEC
E1	7.8744 (00:31:29.9)	-43.0096 (-43:00:34.6)
E2	9.5000 (00:38:00.0)	-43.9980 (-43:59:52.8)
S1	42.8200 (02:51:16.8)	0.0000 (00:00:00.0)
S2	41.1944 (02:44:46.7)	-0.9884 (-00:59:18.2)
C1	54.2743 (03:37:05.8)	-27.1116 (-27:06:41.8)
C2	54.2743 (03:37:05.8)	-29.0884 (-29:05:18.2)
C3	52.6484 (03:30:35.6)	-28.1000 (-28:06:00.0)
X1	34.4757 (02:17:54.2)	-4.9295 (-04:55:46.2)
X2	35.6645 (02:22:39.5)	-6.4121 (-06:24:43.6)
X3	36.4500 (02:25:48.0)	-4.6000 (-04:36:00.0)

2.2 OBSTAC

During the course of the season a variety of weather, seeing, and sky-brightness (Moon) conditions are expected to occur. A computer application, the “Observer Tactician” (ObsTac) [21] uses this information to select the highest priority fields to observe during the next 15 minute interval throughout the night. A simplified version of the ObsTac decision tree is shown in Fig. 3. On the first night of the survey ObsTac will prefer to select SN fields because all of those will not have been observed in the previous 6 nights. In practice ObsTac waits for those fields to rise. An “Exposure Table” keeps track of those images that have been completed. ObsTac selects the highest-priority wide-field images left to complete, where priority includes whether the field is approaching the air-mass limit of 1.4.

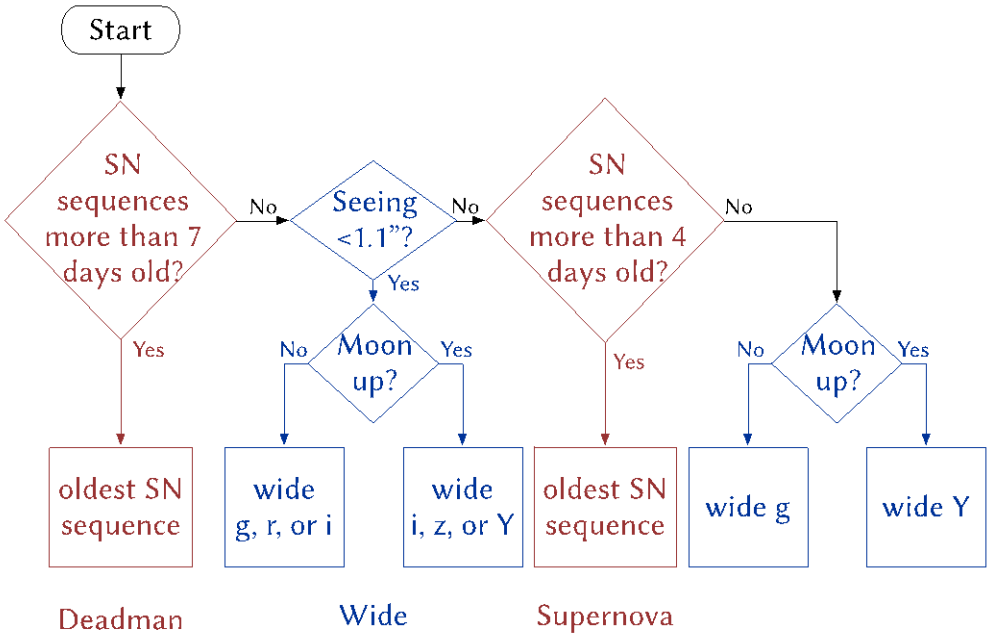

Figure 3. A simplified version of the scheduling algorithm implemented by the Observer Tactician algorithm “ObsTac”. The “seeing” is that expected based on current conditions when projected to an equivalent i-band observation taken at zenith. “wide” is short for “wide-field” observations.

2.3 Observation Schedule & Staffing

The DES observations are staffed by collaboration members and are done at the telescope. The Operations Scientist schedules the observing team. There are three observing roles during full nights. "Observer 1" controls the camera through the data-acquisition interfaces [6] and executes the nightly program by following standard DES observing procedures [22]. This observer ensures that images are being recorded, pays attention to the alarms and warnings, and solves routine problems where procedures have been established. "Observer 2" performs quality control procedures, checks the images for problems and ensures that the image quality is as expected given the current conditions. The "Run Manager" is the lead observer and is responsible for ensuring that the two other observers understand how to perform their roles. The Run Manager also has some daytime responsibilities described below, so they are not expected to stay up for the full night. During half-night observations we usually have two observers with the Run Manager taking on one of the roles. Sometimes there are additional observers due to overlapping travel schedules and when we want to have increased observer training.

Generally, the "Observer 1" role can be performed by an inexperienced but attentive observer. We often fill these positions with students and post-docs who have no previous observing experience. We prefer to have more-experienced observers as "Observer 2" for their expertise in image quality. Run Managers are required to have performed both observing roles effectively.

Support is available to the observers through the CTIO Telescope Operator (on hand), the CTIO Observer Support Specialist (on-site), the CTIO Instrument Scientist (typically by phone), and the DES Operations Support Team (by internet connection).

2.4 Daily Operations Cycle

The typical [23] "Daily Cycle" starts with the Run Manager's Meeting held daily at 16:00 CTIO time. The Run Manager meets by phone with the Operations Support and Data Management [24] (DESDM) Teams. We discuss any technical or procedural problems that occurred during the previous night, provide additional information to DESDM about individual images that might be problematic (for example, if the telescope slewed during the image), receive the DESDM-calculated data quality from previous night's imaging (see Section 2.5), and discuss what to expect from ObsTac based on the expected weather conditions. After this meeting the Run Manager implements the data quality, updating the Exposure Table so that ObsTac has up-to-date information on which images need to be redone.

The period before twilight is used for calibrations and to establish the basic functionality of the instrument. An LED system [25] illuminates a flat-field screen attached to the inside of the dome. We take a set of biases and flats in each of the filters. These images are used in the daily calibration. An hour before sunset the telescope operator will open the dome. At minus 10 degree twilight (roughly 40 minutes after sunset) the observers execute three standard star field [26] exposure scripts, one at high airmass (X=1.65 to 2.1), one at medium airmass (X=1.25-1.65), and one at low airmass (X<1.25). At minus 12 degree twilight (roughly 48 minutes after sunset) the observers begin ObsTac observations. These continue during the night until minus 10 degree morning twilight, for standard star observations, and finally dome flats. In addition to the nightly standard star observations, a) an all-sky infrared camera [27] measures the distribution and amount of water in the atmosphere, b) a GPS receiver mounted on one of the small domes at CTIO measures the amount of water vapor, and c) during some of the observations a 4-narrow-band filter camera system [28] was used to monitor precipitable water vapor and aerosols in the atmosphere. This information is used in the final calibration process.

The observers maintain commentary and notes in an electronic logbook. At the end of each night the observers create two night summaries. The "CTIO Night Report" lists weather conditions, problems encountered, and the fraction of time lost to each. The "DES Night Summary" provides the narrative of the shift including the expected plan with ephemeris, the conditions, accomplishments, problems encountered, and notes for the DESDM team. A series of automatically generated plots and statistics follows, including transparency, PSF, and ellipticity of stars for each image, a note of any gaps between exposures of greater than 60 seconds, the progress on wide-field and SN surveys (figures similar to those shown in Section 4), and a list of exposures. This summary provides a concise history of what happened during that particular night.

The images are transferred by the NOAO Data Transport System [29] (DTS) to NCSA/UIUC in Urbana-Champaign, Illinois, usually within 5 minutes after the moment that the shutter closed. Copies of the data are stored in La Serena and at the NOAO Science Archive in Tucson [30]. To conserve both disk space and network bandwidth the DECam data are losslessly FITS tile-compressed [31] using FPACK. Note that both the DESDM pipeline, described below, and the Community Pipeline [32] use a lossy FPACK compression [33].

The camera and telescope are returned to a safe condition after observations are finished.

2.5 Data Processing & Data Quality

The DESDM pipeline performs image detrending and calibration that we referred to as "First Cut" in order to assess the quality of each exposure with respect to the minimum requirements necessary for DES to obtain its scientific objectives. The overscan and bias is subtracted and the image is divided by the mean dome flat. The CCD crosstalk is removed using a premeasured matrix, a linearity correction applied, fringe and pupil ghost corrections are combined, and a star flat is applied to subsections on each CCD. An astrometric solution for each image is found by comparing to known stellar positions in the 4th USNO Astrograph Catalog (UCAC-4) [34]. Finally, the point spread function (PSF) is determined by examining the shapes of stellar images and then the position, brightness, and rudimentary shape of objects detected in each image are cataloged.

We determine if the image is adequate for the wide-field survey by requiring that the "Effective Time", $t_{effective}=(0.9k/FWHM)^2(Bkgd_{dark}/Bkdg)(10^{-2C/2.5})$ exceeds a minimum. Here k is a filter-dependent "Kolmogorov Factor" scaled relative to i-band that takes into account the natural seeing dependence on wavelength, FWHM is the delivered point-spread-function for stars, Bkgd and $Bkgd_{dark}$ are the measured sky background and dark sky condition, and C is the atmospheric extinction offset calculated from a comparison of the brightness of stars within the image to those in the APASS DR7 and/or NOMAD public catalogs [35-36]. We require that $t_{effective} > 0.2$ for g, and Y-bands and > 0.3 for r, i, and z-bands. Each image is then checked for artifacts, such as satellites and airplane trails, and these images are flagged.

Supernovae are discovered by searching for temporal variations in brightness between SN template images and SN exposures. These SN search images are first processed through a detrending pipeline similar to First Cut, and then through a difference imaging pipeline. The SN difference imaging pipeline aligns the template and search images, adjusts the template image to match the seeing conditions of the search image, then subtracts the two images to produce a "differenced" image. Object detection software runs over the differenced image to identify transient objects, these transient objects are then passed through machine learning algorithms and human scanning to identify transients which are supernova candidates. The data quality and the efficiency of this pipeline is monitored by inserting fake supernovae into the search images and monitoring how well these fake events are recovered by the pipeline. In particular, four fake supernovae of fixed magnitude (magnitude 20) are inserted into each CCD in each search image. The search images are considered to be of acceptable quality if > 90 % of the fixed magnitude fakes is recovered and the S/N of the magnitude 20 fakes is > 20 for shallow fields and > 80 for deep fields. There is an additional requirement that seeing is < 2.0 arc seconds if projected to i-band at zenith instead of the filter/airmass combination of the exposure.

The First Cut processing and data quality evaluation and the SN image pipeline are typically turned around in 2 to 3 days. The results are applied to the Exposure Table by the Run Manager as described in the previous subsection.

3. Y1 EFFICIENCY & LOSSES

3.1 Efficiency from CTIO Night Reports

The CTIO Night Reports (see Section 2.4) were collated to produce the estimate of efficiency shown in Table 2. Of the approximately 890 hours of potential observing time, DES lost 10.2% due to weather that was bad enough that the dome did not open (mostly during September and October), and just under 5% due to problems with the camera or telescope. A tiny amount of time was lost due to "observer error" (perhaps that means that the procedures need an increase in font size).

The time lost due to the camera or telescope failures was dominated by two incidents. A night was lost during October due to a software error in the Telescope Control System. A night was lost during November when it was realized that a

CCD on the focal plane was not responding correctly to clock signals. Subsequent investigation showed that it had failed. This is the second CCD on the focal plane that has failed since installation. The first failed in November 2012 because of exposure to the morning twilight sky. Both broken CCDs are on the outside edge of the array. Oddly, they are opposite to each other; symmetry has been restored to the CCD array. Most of the remainder of the lost time is a number of minor delays in observing due to computer interface and software problems. We are working with CTIO to reduce [37] the frequency of these glitches. There were occasional problems with the encoders that report the dome position, which resulted in partially occluded primary mirror. These were eliminated in December 2013 when CTIO installed a new dome position encoder system. Finally, roughly once per night a shutter hardware error occurred, at the cost of an image plus about a minute of recovery time. Though this was not a major factor in lost observing time, it indicated a potential for a serious hardware failure (and substantial downtime). DES arranged for the shutter repair, and performed regular servicing of the filter changer mechanism in March 2014, after Y1 had been completed.

Table 2. DES Operational efficiency sums accumulated through Y1. These are based on the observer's reports in the CTIO Night Summaries. Time Available is the time we should spend with the shutter open. Observing time is the number of hours the observers were engaged in observing. Next is indicated the number of hours lost to bad weather that results in closing the dome instead of observing, to a failure of the telescope, dome, or mountaintop infrastructure, to the camera, and to obvious observer error.

Operation	**DES Yr. 1 Accumulated Hrs.**	**(%)**
Observing Time Available	888.25	100
Observing Time	751.50	84.6
Bad Weather	90.25	10.2
Telescope or Infrastructure Failure	18	2.0
Camera Systems Failure	25.75	2.9
Observer Error	2.75	0.3

3.2 Open Shutter Efficiency

A second measure of the efficiency is determined from the exposure history. A sum of the open-shutter exposure time compared to elapsed time is calculated from the start of the first ObsTac image to the end of the last on a given night. That calculation indicated we performed ObsTac observing for 548.6 out of 870.1 hours, amounting to 63% of the nights. The time between shutter-closed and shutter-open was 26s to 30s when there was no telescope slew. Slews required additional time. The open-shutter efficiency increased by about 4% during January and February 2014 after the dome encoders were replaced. From then on, if there was a slew to a new position, the settling-time of the telescope determined when we could open the shutter.

3.3 DIMM & Delivered Seeing

During planning for the survey we expected the camera and telescope would degrade the image quality by approximately 0.55" in quadrature with the night's optimal site seeing. Y1 started with nights with cold air temperatures. We found that the image quality was not as expected from the CTIO DIMM. See Fig. 4. ObsTac responded (correctly) by taking g-band and Y-band images in the condition shown on the RHS edge of Fig. 3. This was alarming and of increasing concern to DES. Towards the end of October it was discovered that the dome floor cooling was not functioning well (floor was warm compared to the ambient air). In early November CTIO made the primary mirror cooling more aggressive by running it all day (instead of just a part of the afternoon) and repaired the floor cooling. At about the same time the weather warmed up.

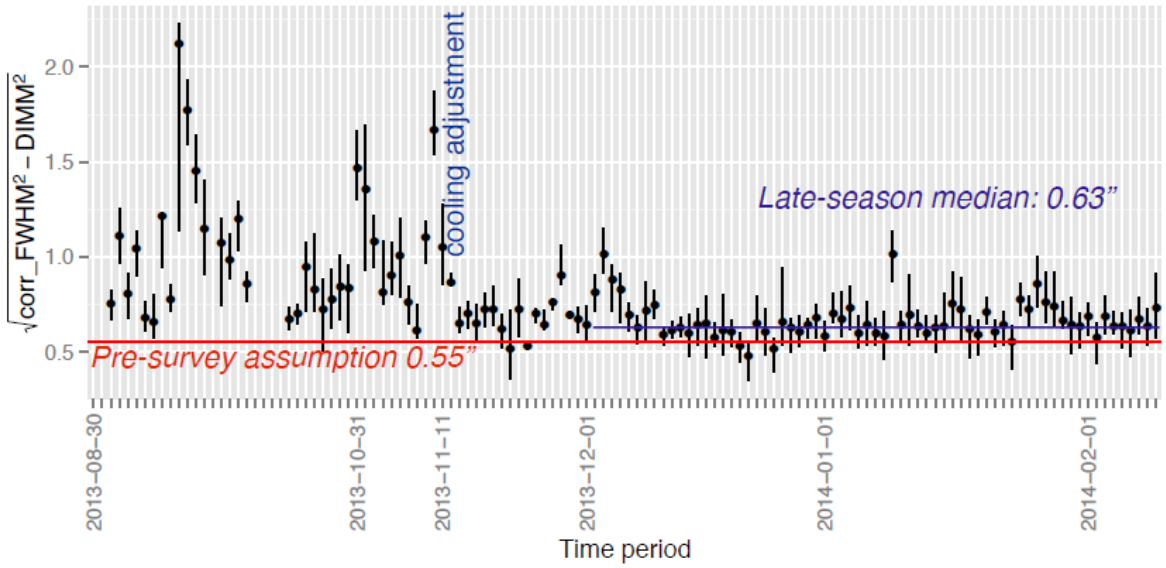

Figure 4. The difference in arc-seconds between the DECam-delivered seeing, corrected to zenith, and the site-seeing as determined from the CTIO DIMM for each survey night. The red line, at 0.55”, is what we expected during the survey design. The improvements to the dome floor cooling and primary mirror cooling algorithm were made by the afternoon of the indicated date.

4. WIDE FIELD AND SUPERNOVA SURVEY PROGRESS IN DES YEAR 1

4.1 Wide Field Survey Progress

In total we recorded 17671 WF images. Of those, 82% passed the $t_{effective}$ data quality measure. Of the 18% that were declared “unusable”, 78% were recorded before the changes to the dome floor and primary mirror cooling and the weather warmed up. The bulk of the bad exposures were g- and Y-band exposures directed by ObsTac during poor achieved seeing. Fig. 5 shows the number of good exposures in each of the four Y1 tilings for each of the five filters. Fig 5 shows we successfully covered the eastern part of the Y1 field with four tilings in all five filters. Fig. 5 also shows that there are survey areas in the western part of the Y1 field where we did not achieve four tilings in each filter (because of the early seeing struggles), that there are areas in Stripe 82 where we did not achieve any tilings in dark-time filters (due to the proximity of the Moon), and that there is a considerable part of the eastern Y2 area that was finished in Y1, especially in z- and Y-band (because we ran out of accessible Y1 targets in the latter weeks of the Y1 observing season). We have successful exposures in 82% of the Y1 field and 16% of the Y2 fields as of the end of Y1.

The seeing achieved in the Y1 WF exposures is shown in Fig. 6. The g- and Y-band (LHS) exposures that passed the $t_{effective}$ DQ criterion had a median FWHM of 1.17”. The histogram shows features consistent with exposures being taken under the two different ObsTac observing criteria for g- and Y-band. That there were so many more unusable exposures taken in g- and Y-band is a further consequence of ObsTac, for as we noted in Section 2.2, ObsTac schedules g- and Y-band exposures when the seeing is poor. The good r-, i-, and z-band exposures (RHS) had a median seeing of 0.94”. The survey goal in this latter set of filters is a median seeing of 0.90” or better.

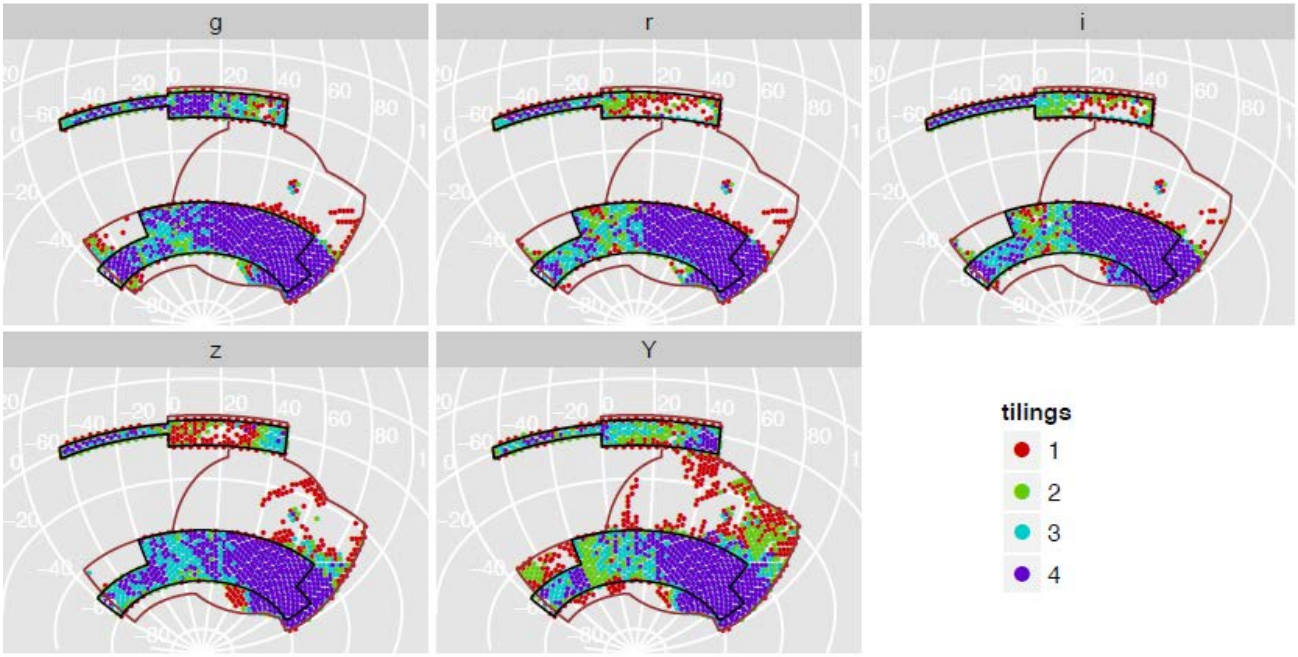

Figure 5. The Y1 survey fields include Stripe 82 (at the Equator), and the boxed-in area at roughly -40 < RA < -60 degrees. There was a maximum of four tilings in each filter. The colored dots represent the number of "good" exposures (as defined by the $t_{effective}$ data quality criterion described above) achieved in each filter.

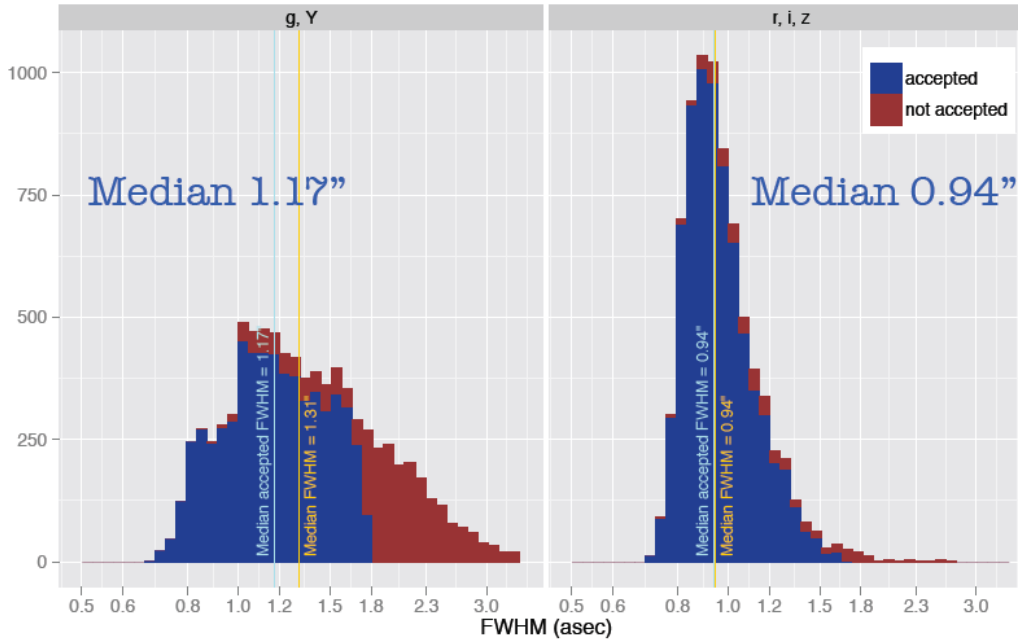

Figure 6. The seeing for WF images in DES Y1. The left hand side plot shows the FWHM versus number of exposures for the combined g-, and Y-band data. The blue (brown) histogram is for exposures that passed (failed) the $t_{effective}$ criterion. The right hand side plot shows similar information for the combined r-, i-, and z-band exposures.

4.2 Supernovae Survey

We recorded 2699 SN-sequence exposures during Y1. Of these 95% passed the SN data quality threshold described in Section 2.5. Fig. 7 shows the nights on which we observed each SN sequence for the 10 SN fields. Note, again, that the C3 and X3 fields are the deep fields. For those two fields there are four "sequences" each, defined on a filter-by-filter basis, whereas for the shallow fields a sequence is comprised of all of the exposures in the four filters. The biggest gaps in the SN sequences are in mid-October when there was an 8-day engineering period and late-November across a period with five nights of non-DES observing followed by a DES night lost because the camera was off-line. These gaps are summarized in Fig. 8, which shows the mean, median, and maximum gap for each sequence. We note that when the weather is perfect these will be observed with at least six-night gaps. We found roughly 1700 SN candidates of all types in Y1 [38].

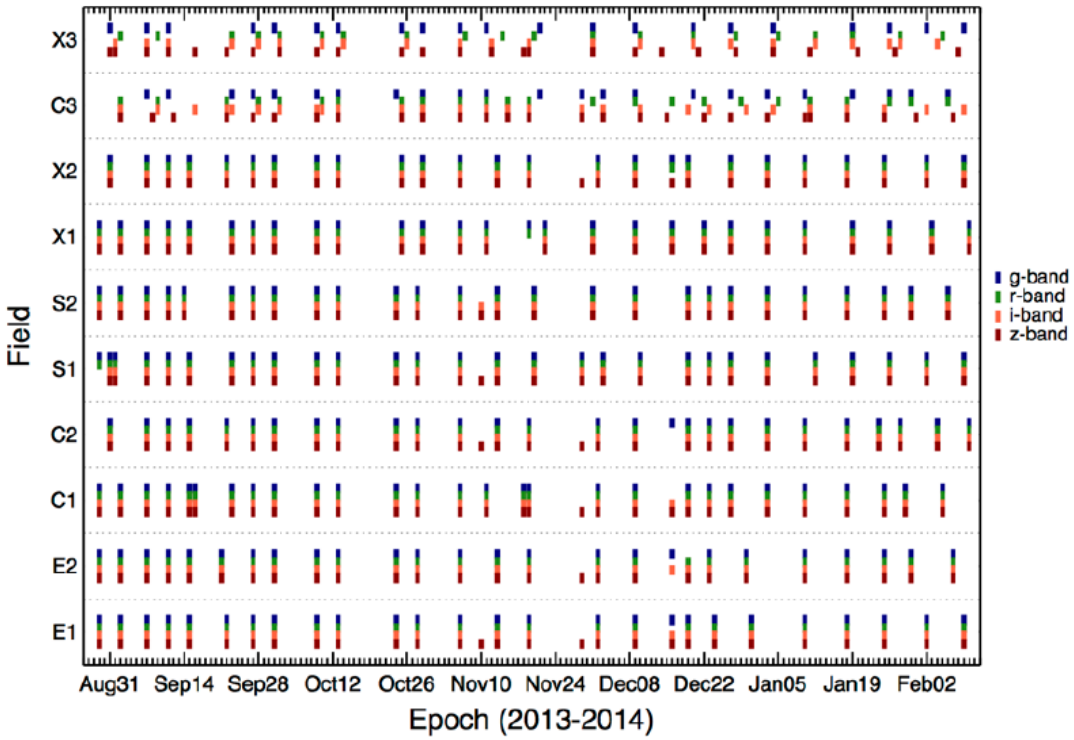

Figure 7. The DES Year 1 SN observations. The horizontal axis is the date from August 15, 2013 to February 10, 2014. The vertical axis lists each of the 10 SN fields. If the SN field was observed there is a vertical bar with a separate color block for each filter. The two "deep fields" are C3 and X3.

5. YEAR TWO OUTLOOK AND PLAN

The goal of DES observing season two (Y2) is to finish the WF observations for the first four tiles of the 5000 square-degrees survey. That is, we plan to finish the unobserved parts of the Y1 field and observe the complement of the field outlined in Fig. 2. We performed detailed simulations of the Y2 observing schedule that took into account variants in the weather based on historical data, expected data quality, the distribution of bright and dark time, and included constraints on the total number of nights and balance of bright/dark time. The metric used for evaluation was the number of completed survey quality exposures. Our request is for 105 nights starting in mid-August with 2nd half-nights. In mid-September we would transition to full nights. In mid-December we would transition to 1st-half nights and continue until roughly the beginning of February 2015. This differs from Y1 in that there are significantly more half nights, an improvement because 1st half-nights early in the season and 2nd half-nights late in the season are not very useful due to the location of the survey footprint. We requested that non-DES blocks of time, including engineering time, be no longer than three nights during grey or dark time or five nights around the full Moon to reduce the gaps in the SN cadence.

Unless we make operational improvements we expect to fall approximately 10% short of our goal for Y2.

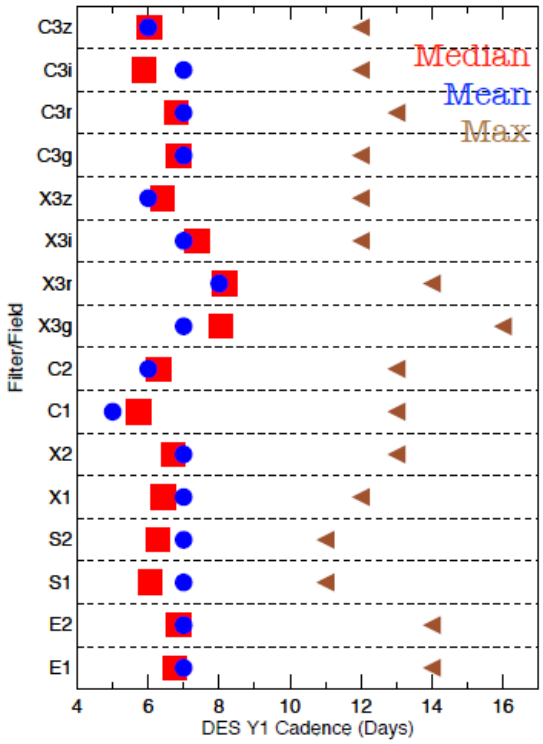

Figure 8. The mean, median, and maximum gaps (observer frame) between successful SN sequences during Y1.

5.1 Improvements Expected in Y2

In between Y1 and Y2 CTIO will continue to improve telescope operations and these upgrades will directly benefit DES (and all the other DECam observers).

Better control of the air temperature within the Blanco dome will be achieved by the addition of two large glycol-cooled air handling units at the level of the telescope. These have been installed as of the time of this conference. Operational parameters of the environmental controls systems will be tuned. The goal is to have the primary mirror slightly cooler than the surrounding air while nighttime observations are underway, with minimal air stratification in the dome, and with the inside and outside temperatures being the same.

The Blanco primary mirror support system as now implemented presents forces to the primary depending on the gravity vector, plus a static astigmatism correction. Data taken in 2013 ascertained that it is possible to improve the mirror figure as a function of sky position so as to better zero-out primary mirror aberrations. To achieve active control of the primary mirror figure requires that CTIO install high-resolution primary mirror support transducers and controls. The prototype was installed and tested in January 2014. Fabrication of a complete system is underway. These will be installed by September 2014.

Additional diagnostic instrumentation has been installed during Y1. Sensitive accelerometers were added to the telescope structure and a Doppler anemometer was installed near the camera. CTIO and DES are analyzing the new data to better understand telescope motions and to optimize the usage of the wind-blinds.

The handshake between the telescope controls and the camera controls can be improved to shave a couple of seconds off the time between shutter-close and shutter-open when there has been no slew between exposures. The ObsTac algorithm will be tuned to take advantage of this, thus increasing the open-shutter efficiency.

6. SUMMARY

The Dark Energy Survey Collaboration aims to study the accelerating expansion of the Universe through four complementary techniques. To produce the deep, 5000 square-degree survey and the 30 square-degree time-domain SN survey that are specified by the science goals, the collaboration designed and built the Dark Energy Camera, now operating on the Blanco Telescope at CTIO.

DES has completed the first of five 105-night observing seasons. Operational procedures developed for Y1 achieved high survey efficiency. Although there were initial difficulties with image quality related to the cold weather, Y1 was a very good start to the survey and we are encouraged by the tremendous amount of high quality exposures that we eventually recorded. The first scientific results of the survey are being shown [38-40] in public conferences and publications are beginning [18] to be submitted to journals. There is every indication that DES will successfully complete its scientific agenda. The start of Y2 is coming soon. An improved survey strategy combined with upgrades and improvements at the telescope leave us optimistic about the coming observing season.

Fig. 9 shows a composite 3-color image of one of the DES SN fields. It is the field-of-view of one exposure.

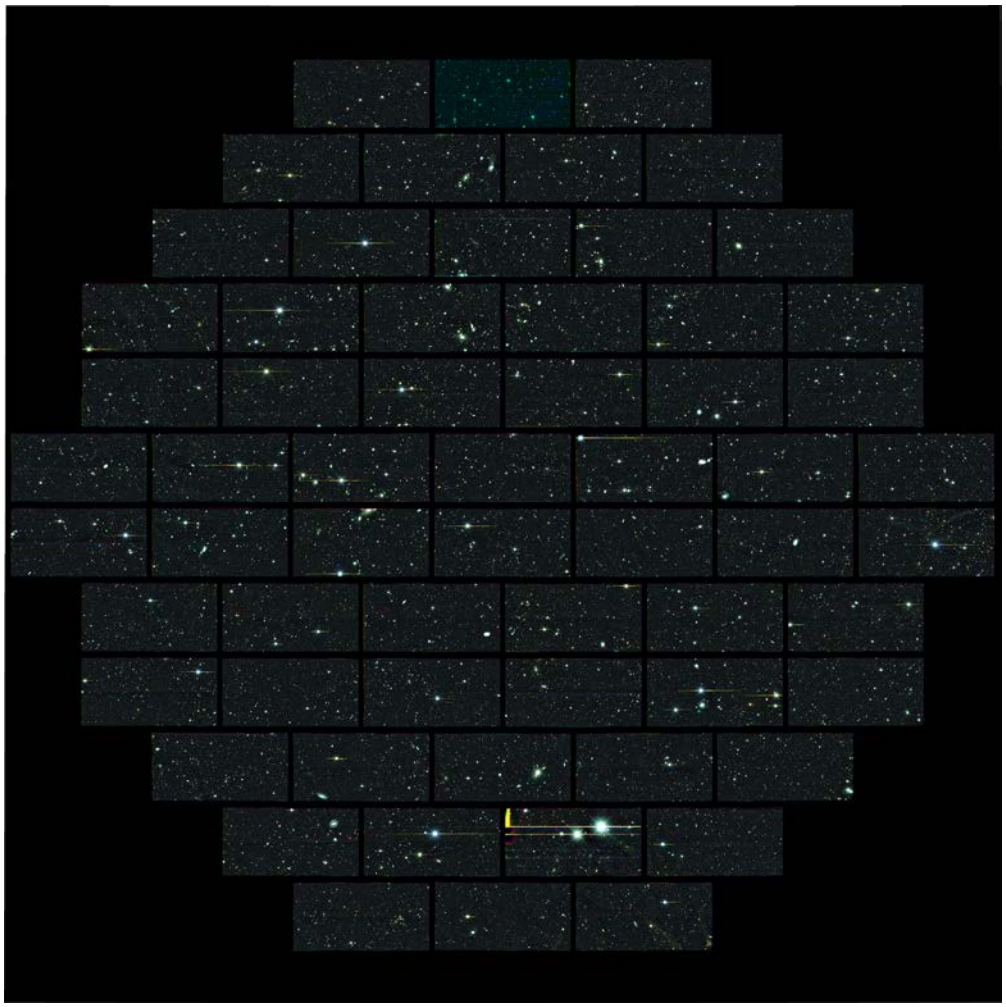

Figure 9. A 3-color composite image of one of the DES SN fields showing the 62 CCDs on the DECam focal plane. It has the field-of-view of one exposure.

ACKNOWLEDGEMENTS

Funding for the DES Projects has been provided by the U.S. Department of Energy, the U.S. National Science Foundation, the Ministry of Science and Education of Spain, the Science and Technology Facilities Council of the United Kingdom, the Higher Education Funding Council for England, the National Center for Supercomputing Applications at the University of Illinois at Urbana-Champaign, the Kavli Institute of Cosmological Physics at the University of Chicago, Financiadora de Estudos e Projetos, Fundação Carlos Chagas Filho de Amparo à Pesquisa do Estado do Rio de Janeiro, Conselho Nacional de Desenvolvimento Científico e Tecnológico and the Ministério da Ciência e Tecnologia, the Deutsche Forschungsgemeinschaft and the Collaborating Institutions in the Dark Energy Survey.

We are grateful for the extraordinary contributions of our CTIO colleagues and the DES Camera, Commissioning and Science Verification, and Operations Support teams in achieving the excellent instrument and telescope conditions that have made this work possible. The success of this project also relies critically on the expertise and dedication of the DES Data Management organization. We are grateful for the administrative and organizational assistance provided by Connie Lang (FNAL) and Ximena Herreros (CTIO).

The Collaborating Institutions are Argonne National Laboratories, the University of California at Santa Cruz, the University of Cambridge, Centro de Investigaciones Energeticas, Medioambientales y Tecnologicas-Madrid, the University of Chicago, University College London, the DES-Brazil Consortium, the Eidgenoessische Technische Hochschule (ETH) Zurich, Fermi National Accelerator Laboratory, the University of Edinburgh, the University of Illinois at Urbana-Champaign, the Institut de Ciencies de l'Espai (IEEC/CSIC), the Institut de Fisica d'Altes Energies, the Lawrence Berkeley National Laboratory, the Ludwig-Maximilians Universität and the associated Excellence Cluster Universe, the University of Michigan, the National Optical Astronomy Observatory, the University of Nottingham, the Ohio State University, the University of Pennsylvania, the University of Portsmouth, SLAC National Accelerator Laboratory, Stanford University, the University of Sussex, and Texas A&M University.

REFERENCES

[1] Abbott, T., et al., “The Dark Energy Survey”, http://arxiv.or/astro-ph/0510346.
[2] Flaugher, B., “The Dark Energy Survey”, Int. J. Modern. Phys. A20, 3121 (2005).
[3] Flaugher, B. L., et al., “Status of the Dark Energy Survey Camera (DECAM) Project”, Proc. SPIE Vol. 8446, 844611 (2012).
[4] Diehl, H. T., For the Dark Energy Survey Collaboration, “The Dark Energy Survey Camera (DECAM)”, Physics Procedia v. 37, 1332 (2012) and references therein.
[5] Shaw, T. et al., “The Dark Energy Camera Readout System”, Proc. SPIE 8453, 84532Q (2012).
[6] Honscheid, K. et al., “The Readout and Control System of the Dark Energy Camera”, Proc. SPIE 8451, 845112 (2012).
[7] Doel, P., et al., “Assembly, alignment, and testing of the DECam wide field corrector optics”, Proc. SPIE 8446, 84466F (2012).
[8] Holland, S. E., Dawson, K., Palaio, N. P., Saha, J., Roe, N. A., Wang, G., "Fabrication of back-illuminated, fully depleted charge-coupled devices," Nucl. Instrum. Methods **A 579**, 653-657 (2007).
[9] Diehl, H. T., et al., “Testing the Dark Energy Camera on a Telescope Simulator”, Proc. SPIE 7735, 7735-125 (2010).
[10] Soares-Santos, M., et al., “The Dark Energy Camera Integration Tests on a Telescope Simulator”, Physics Procedia v. 37, 1445 (2012).
[11] Derylo, G., et al., “Transport and Installation of the Dark Energy Survey CCD imager”, Proc. SPIE Vol. 8446, 84466J (2012).
[12] Abbott, T. M. C. A., “Dark Energy Camera Installation at CTIO: Overview”, Proc. SPIE 8444, 844445 (2012).
[13] Munoz, F, “Dark Energy Camera installation at CTIO - Technical challenges”, Proc. SPIE 8444, 844446 (2012).
[14] Cease, H., et al., “Commissioning and Initial Performance of the Dark Energy Camera Liquid Nitrogen Cooling System”, Proc. SPIE 8446, 8446-259 (2012).

[15] Among those present at “First Light” on September 12, 2012 were Tim Abbott, Alistair Walker, Chris Smith, Mauricio Rojas, David Rojas, M. Martin, Darren DePoy, Brenna Flaugher, Marcelle Soares-Santos, Steve Kent, Theresa Shaw, Herman Cease, and Tom Diehl. Many people attended by internet communication including Nicole van der Bliek, David James, Klaus Honscheid, Josh Frieman, Adam Sypniewski, and Juan Estrada.
[16] Roodman, A., “Focus and alignment of the Dark Energy Camera using out-of-focus stars”, Proc. SPIE 8446, 84466O (2012).
[17] Roodman, A. J., Reil, K., Davis, C., “Wavefront sensing and the active optics system of the Dark Energy Camera”, these proceedings.
[18] Melchior, P., et al., “Mass and galaxy distributions of four massive galaxy clusters from Dark Energy Survey Science Verification data”, arXiv:1405.4285.
[19] Ruhl, J. E., et al., “The South Pole Telescope”, Proc. SPIE 5498, 5498-11 (2004).
[20] Annis, J., et al., The SDSS Coadd: 275 degrees-squared of Deep SDSS Imaging on Stripe 82”, arXiv:1111.6619.
[21] Neilsen, E., and Annis, J., “ObsTac: automated execution of Dark Energy Survey observing tactics”, FERMILAB-CONF-13-397-CD.
[22] https://cdcvs.fnal.gov/redmine/projects/desops/wiki
[23] Reil, K. A., et al., “Typical Day at DES”, these proceedings.
[24] Mohr, J. J., et al., “The Dark Energy Survey Data Processing and Calibration System”, Proc. SPIE 8451, 8451-0D (2012).
[25] Rheault, J.-P., et al., “Spectrophotometric calibration system for DECam”, Proc. SPIE 8446, 84466M (2012).
[26] Tucker, D. L., et al., in ASP Conf. Ser. Vol. 364, The Future of Photometric, Spectrophotometric and Polarimetric Standardization, Astron. Soc. Pac., ed. Sterken C., San Francisco, 187 (2007).
[27] Reil, K. A., Lewis, P., Schindler, R. H., “The Radiometric All-sky Infrared Camera (Rasicam)”, these proceedings.
[28] Li, T., et al., “Monitoring the atmospheric throughput at Cerro Tololo Inter-American Observatory with aTmCam”, Proc. SPIE 9147, 9147-262 (2014); these proceedings.
[29] Fitzpatrick, M. J., “DTS: The NOAO Data Transport System”, Proc. SPIE 7737, 77371T (2010).
[30] http://portal-nvo.noao.edu
[31] Pence, W. D., Seaman, R., & White, R. L., “Lossless Astronomical Image Compression and the Effects of Noise”, PASP 121, 414 (2009) and http://heasarc.nasa.gov/fitsio/fpack.
[32] Smith, R. C., Walker, A. R., and Miller, C., “DECam Community Pipeline Software requirements and technical Specifications”, http://www.noao.edu/meetings/decam/media/community_pipeline.pdf.
[33] Pence, W. D., White, R. L., & Seaman, R., “Optimal Compression of Floating-point Astronomical Images without Significant Loss of Information”, PASP 122, 1065 (2010).
[34] Zacharias, N., et al., Astronomical Journal **145**, 44 (2013).
[35] Hendon, A. A., et al., JAAVSO **40**, 430 (2012) and http://www.aavso.org/apass.
[36] http://www.ap-i.net/skychart/en/news/nomad.
[37] Honscheid, K., “Lessons learned: reviewing the DECam data acquisition system after one year in service”, Proc. SPIE 9152, 9152-14 (2014); these proceedings.
[38] March, M., for the Dark Energy Survey Collaboration, “Initial supernovae results from the Dark Energy Survey”, Invited Talk at the APS March Meeting, Denver, CO, 2014.
[39] Clampitt, J., for the Dark Energy Survey Collaboration, “Weak Lensing in the Dark Energy Survey”, Invited Talk at the APS March Meeting, Denver, CO, 2014.
[40] Rozo, E., for the Dark Energy Survey Collaboration, “Early results on Galaxy Clusters from the Dark Energy Survey”, Invited Talk at the APS March Meeting, Denver, CO, 2014.